Nanoscale

Cite this: *Nanoscale*, 2011, **3**, 2301

www.rsc.org/nanoscale

PAPER

Strain-induced magnetic transitions in half-fluorinated single layers of BN, GaN and graphene

Yandong Ma, Ying Dai,* Meng Guo, Chengwang Niu, Lin Yu and Baibiao Huang

Received 14th February 2011, Accepted 24th March 2011
DOI: 10.1039/c1nr10167f

Recently, extensive experimental and theoretical studies on single layers of BN, GaN and graphene have stimulated enormous interest in exploring the properties of these sheets by decorating their surfaces. In the present work we discuss half-fluorinated single layers of BN, GaN and graphene, in the context of intercoupling between strain and magnetic property. First-principles calculations reveal that the energy difference between ferromagnetic and antiferromagnetic couplings increases significantly with strain increasing for half-fluorinated BN, GaN and graphene sheets. More surprisingly, the half-fluorinated BN and GaN sheets exhibit intriguing magnetic transitions between ferromagnetism and antiferromagnetism by applying strain, even giving rise to half-metal when the sheets are under compression of 6%. It is found that the magnetic coupling as well as the strain-dependent magnetic transition behavior arise from the combined effects of both through-bond and *p–p* direct interactions. Our work offers a new avenue to facilitate the design of controllable and tunable spin devices.

I. Introduction

Light element magnets hold great promise to overcome the limitations of technologies depending on current magnetic materials based on *d* and *f* elements as they involve only *sp* elements. This topic has captured a rapid surge of interest since magnetism was experimentally observed in polymeric fullerenes[1] and graphite.[2] Despite great theoretical efforts, the predicted magnetism is mostly induced by localized electron states in a variety of zero-,[3,4] two-dimensional (2D),[5–7] and bulk[8,9] metal-free materials. Nevertheless, for the application of nano-electronics, nanoscale magnets with tunable spin ordering are more desirable. This requires that the magnetic coupling among the polarized electron spins can be convenient to control in nanostructures.

Such ferromagnetic (FM) coupling has been observed in BN nanotubes (BNNTs) with fluorination,[10,11] in which the spin polarization exhibits remarkable radius dependence and thus it is convenient to control. It is demonstrated that the relatively weak FM ordering in F-BNNTs can be enhanced by increasing local tube curvature.[10,11] In analogy to BNNTs, BN nanosheets (BNNSs) are of interest due to their unique properties, such as high thermal stability and chemical inertness. However, just opposite to BNNTs, half-fluorinated BNNSs have been found to possess distinct magnetic properties, namely antiferromagnetic (AFM) couple.[12] This difference as well as the radius-dependent behavior of BNNTs is related to the strain caused by curvature effects. Thus, it becomes much intriguing if the relative stability of FM and AFM spin orders of half-fluorinated BNNSs can be modulated by controlling the applied strain. Moreover, modulating spin transport in a well-controlled manner is crucial to actual applications. Alternative approaches of magnetic modulation through external fields[13,14] and doping[15,16] have been proposed in various structures, but in light-element magnets the acquisition of controllable spin ordering remains an important challenge. By analogy, it is attractive to investigate the relevant properties of the half-fluorinated graphene and GaN sheets (GNNSs) to see if they exhibit similar variation by applying strain.

Recently, hydrogenated graphene was predicated to be an electronic insulator in theory,[17] and was verified subsequently by experiment.[18] These studies on graphene stir up significant interest in other honeycomb lattices. For the subsequent intensively studied half-decorated 2D sheets,[12,19–22] its magnetic mechanism is still controversial. For example, according to the currently viewpoints about the magnetism of half-decorated 2D sheets, the magnetic coupling is ferromagnetism.[19–22] However, recent theoretical studies reported that half-fluorinated graphene and BNNSs[12] are AFM semiconductors, which reveals that the existing magnetic mechanisms are not credible in these systems. Accordingly, searching for a reasonable theory is necessary to provide a concise physical understanding of the magnetic mechanism in these materials.

In the present work, we study the strain effects on magnetic properties of half-fluorinated BNNSs, GNNSs and graphene based on first-principles calculations. The results demonstrate that (1) magnetic transitions between FM and AFM in half-fluorinated BNNSs and GNNSs can be induced by introducing

School of Physics, State Key Laboratory of Crystal Materials, Shandong University, Jinan, 250100, People's Republic of China. E-mail: daiy60@sdu.edu.cn; Fax: +86 531 88365569

strain: FM semiconductors under compressive stress of 6%, while AFM semiconductors under tensile stress of 6%; and (2) different from the currently existing magnetic mechanisms,[19–22] we propose an important rule that the magnetism of half-decorated 2D sheet arises from the combined effects of through-bond and *p–p* direct interactions. These findings suggest a new route to facilitate the design of controllable and tunable spintronic devices.

II. Methods

Our calculations are based on the spin-polarized density functional theory (DFT) using generalized gradient approximation (GGA)[23] for exchange–correlation potential. We have used Perdew–Burke–Ernzerhof (PBE) functional for GGA as implemented in the Vienna *ab initio* Simulation Package (VASP).[24,25] For the geometric and electronic structural calculations, a supercell consisting of fourfold unit cells of each single layer is used with a vacuum space of 15 Å between two layers to avoid interactions between them. The Brillouin zone is represented by the set of $9 \times 9 \times 1$ k-points [26] for the geometry optimizations and by that of $17 \times 17 \times 1$ k-points for the static total energy calculations. The energy cutoffs, convergence in energy, and force are set to 400 eV, 1×10^{-5} eV, and 0.02 eV Å^{-1}, respectively. To determine the stability of the half-fluorinated single layer, the formation energy of the fluorinated single layer is estimated by calculating $E_f = (E_{total} - E_{pure} - N_F E_F)/N_F$, where E_{total} is the energy of the half-fluorinated single layer, E_{pure} is that of the pristine single layer, E_F is the binding energy per atom of an F_2 molecule, and N_F is number of adsorbed fluorine atoms.

The accuracy of our calculation is tested using pristine BNNSs, GNNSs and graphene. The optimized structures of BNNSs and GNNSs are graphene-like flat planes. The calculated nearest-neighbor bond length and the lattice constant of BNNSs, GNNSs and graphene are in good agreement with the previous results[27] (as shown in Table 1).

III. Results and discussion

3.1 Geometry and electronic structure

For the convenience of our discussion, we denote the BNNSs, GNNSs and graphene as *ab* (*ab* = BN, GaN and graphene). Usually, the single layers are laid on a substrate,[28] therefore, we consider only one-side fluorination in this work. To determine the most stable structure of the half-fluorinated sheet, we consider three possible adsorbed structures T_A, T_B, and H; the F atoms occupy the ontop positions of all the *a* sites in T_A, those of all the *b* sites in T_B, and all the hollow sites in H. All the initial arrangements of the three structures are fully relaxed, and the formation energies are calculated. For the half-fluorinated *ab* sheet, the T_A structure is most stable (as shown in Fig. 1), and the formation energies are 0.28 eV, −0.61 eV and −1.47 eV for half-fluorinated BNNSs, GNNSs and graphene, respectively. Thus, we only consider half-fluorinated *ab* sheet in which F atoms are attached to *a* atoms in *ab* sheet (termed as F–*ab*). As mentioned above, the *ab* sheet prefers the flat structure. However, for F–*ab* sheets, their stable configurations are buckled, similar to Si hexagonal sheet.[27,29] Their relaxed atomic configurations from both top and side views are shown in Fig. 1, and the corresponding structural parameters are listed in Table 1. As shown in Fig. 1(b), the plane of *a* atoms is sandwiched between the plane of F atoms and the plane of *b* atoms, and all the F atoms are adsorbed on *a* atoms with F–*a* bonds arranged perpendicularly to *ab* plane.

Nitrides and carbides of main group elements can exhibit magnetism by introducing a sufficient number of holes, and this phenomenon arises from the contracted nature of 2*p* states of N and C.[30,31] It is known that F atom possesses strong electron affinity, which enables it loot electrons from *ab*. When *ab* sheet is half-fluorinated, the formation of F-*a* bond generates one hole per unit cell and hence one unpaired spin at each *b* atom. To study the preferred coupling between the magnetic moments of *b* atoms in F–*ab*, we examine the energy for three magnetic configurations: (1) FM coupling; (2) AFM coupling; and (3) nonmagnetic (NM) state. It is found that the ground state of F-BNNSs and F-graphene is AFM, while FM is most favorable for F-GNNSs.

To visualize the distribution of spins on F–*ab*, we plot spin density in Fig. 2, together with the corresponding electronic structures. The calculated spin density distributions for F-*ab*

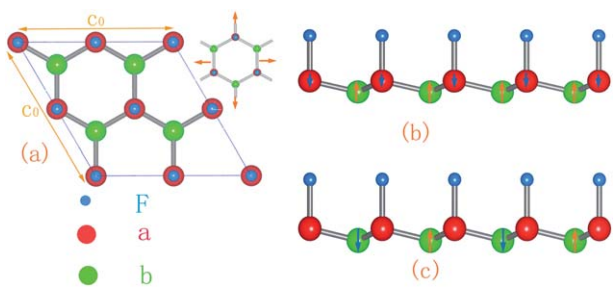

Fig. 1 The optimized geometric structures of half-fluorinated *ab* sheets in top (a) and side (b) views. In the inset, we show that the strain is applied along zig-zag and armchair directions. The mechanism illustration of (b) through-bond spin polarization and (c) *p–p* direct spin polarization.

Table 1 Calculated structure parameters (in Å) of the pristine and half-fluorinated graphene, BNNSs and GNNSs. a, *a-b*, F-*a* and Δ represent the lattice constant, bond length between *a* and *b* atoms, bond length between *a* and F atoms, and buckled height between *a* and *b* layers, respectively

	BNNSs	GaNNSs	graphene	F-BNNSs	F-GNNSs	F-graphene
a	2.51(2.51[a])	3.26(3.20[a])	2.47(2.46[a])	2.64	3.33	2.55
a-b	1.45(1.45[a])	1.88(1.85[a])	1.43(1.42[a])	1.563	1.965	1.50
F-*a*	—	—	—	1.417	1.825	1.494
Δ	—	—	—	0.344	0.405	0.286

[a] Ref. 27.

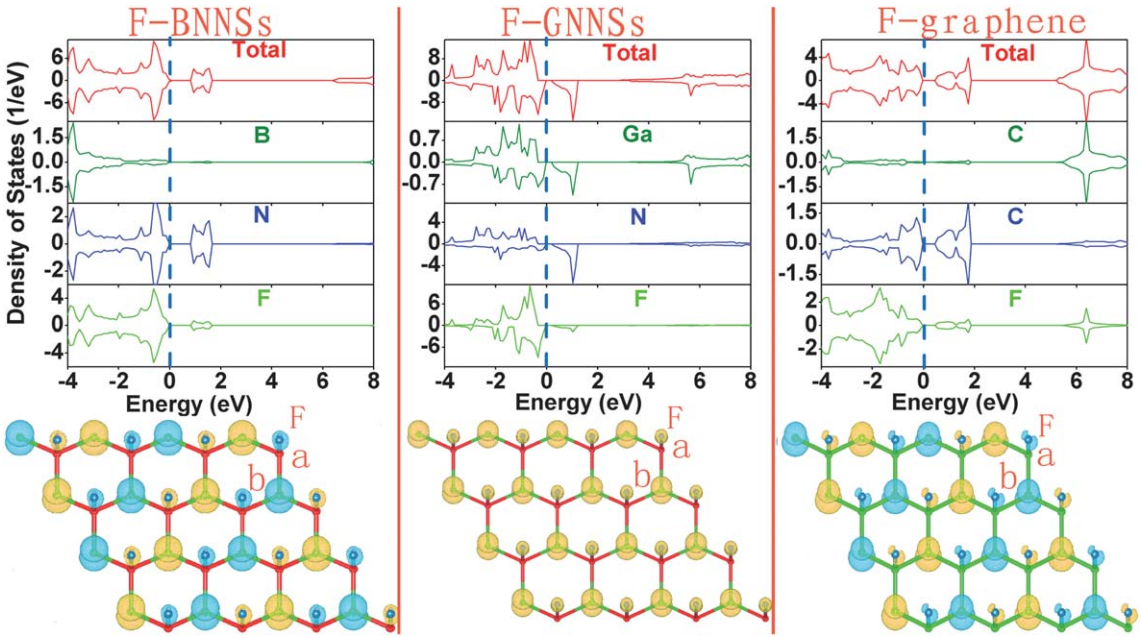

Fig. 2 The spin-resolved charge density isosurface (isosurface value = 0.03 e/Å^3) and DOS of F-*ab* sheets in ground magnetic state. Yellow (cyan) indicates the positive (negative) values. Energies are referred to E_F.

reveal that the magnetic moments are strongly localized on the *b* atoms, as found for other hole-doped nitrides and carbides.[30,31] Examination of the states near Fermi level shows that the magnetic property is mainly contributed by the *p*-electrons of *b* atoms. For F-BNNSs and F-graphene in AFM state, it indicates adsorbed F induces some up-spin and down-spin states above the valence band. For F-GNNSs in FM state, we can see that the spin up channel has a band gap while the spin down channel has partially filled states. The spin polarization, $P = (N_\downarrow(E_F) - N_\uparrow(E_F))/(N_\downarrow(E_F) + N_\uparrow(E_F))$, where $N_\downarrow(E_F)$ and $N_\uparrow(E_F)$ represent the DOS corresponding to the minority and majority spins at the Fermi level, respectively, is calculated to be 100%, which is important for spintronics applications.[32] The major change brought about by the fluorination into F-*ab* sheet is that the down-spin *b* 2*p* states become partially empty.

3.2 Strain-induced magnetic transition between FM and AFM

Strain effect caused by radial size is always important in nanosystems. Previous studies indicated that the spin polarization exhibits remarkable radius dependence in F-BNNTs,[10,11] and increasing local tube curvature can enhance the relatively weak FM order in F-BNNTs.[10,11] Moreover, just opposite to BNNTs, F-BNNSs have been found to exhibit distinct magnetic properties, namely AFM.[12] This difference as well as the radius-dependent behavior of BNNTs is due to strain caused by curvature effects. Motivated by these results, we guess that a nanomechanical modulation of strain can sensitively enhance, quench, or reverse the spin order of F-BNNSs. This would be very practical as strain can be readily exerted on nanosheets either intentionally or naturally. This strategy is also expected to be applicable to other classes of nanosheets, such as F-GNNSs and F-graphene. Here, we investigate the strain dependence of spin order in F-*ab* nanosheets by varying the isotropic strain from −6% to 6%, in which all crystal symmetries and overall honeycomb-like structure are maintained. The tensile or compression strain is uniformly applied along both zig-zag and armchair directions as shown in the inset of Fig. 1a. The isotropic strain is defined as $\varepsilon = \Delta c/c_0$, where the lattice constants of the unstrained and strained supercell equal to c_0 and $c = \Delta c + c_0$, respectively.[33,34] The stretching or compressing of the *ab* sheet is achieved by first elongating the optimized lattice constant c to $c = \Delta c + c_0$ and uniformly expanding the atomic structure obtained from previous optimization. Subsequently, the atomic structure is reoptimized and the corresponding energy is calculated with the elongated lattice constant fixed.

Fig. 3 shows the variation in energy difference ΔE ($\Delta E = E_{FM} - E_{AFM}$) of F-BNNSs, F-GNNSs and F-graphene with strain before and after reoptimization. It is found that the energy difference ΔE increases monotonically with increasing isotropic strain from −6% to 6% for F-BNNSs, F-GNNSs and F-graphene before and after reoptimization. More surprisingly, the magnetic transition between FM and AFM orders in F-BNNSs and F-GNNSs can be induced by applying strain. For the F-BNNSs system under tensile stress, the energy difference ΔE increases with higher tension and the interaction between the fluorination-induced moments keeps AFM. But for the compressive stress on F-BNNSs, with increasing compression, the AFM ordering is rapidly quenched and transforms to FM, and the FM ordering is efficiently enhanced. At 6% compression, FM state is energetically more favorable than AFM state by 87 meV. For the F-GNNSs system under compression stress, the energy difference ΔE decreases with higher compression and the FM state is always more stable than AFM state. While for tensile stress on F-GNNSs, with increasing tensility, the FM ordering is rapidly quenched and transforms to AFM, and the AFM ordering is enhanced. Similar with F-BNNSs, at 6% compress stress, FM state is energetically more stable than AFM state by

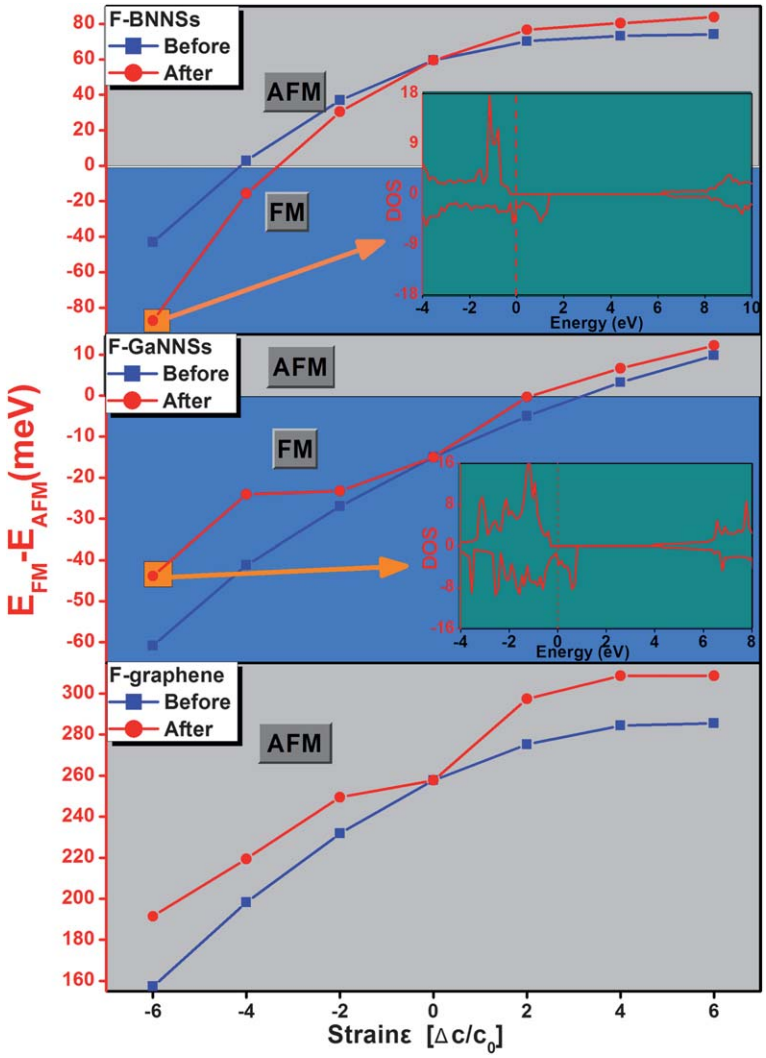

Fig. 3 Strain dependence of the energy difference between FM and AFM order of F-BNNSs, F-GNNSs and F-graphene before and after reoptimization. Blue and gray shaded areas represent the FM and AFM order, respectively. The corresponding DOS of F-BNNSs and F-GNNSs under compressive stress of 6% are illustrated in the insets. The Fermi level is set to zero.

44 meV. The corresponding spin-polarized DOS for both F-BNNSs and F-GNNSs under compressive stress of 6% are illustrated in the insets of Fig. 3, where substantial electronic states are found around the Fermi level for minority spin, while no state is observed for the majority spin. So, electric transport through both F-BNNSs and F-GNNSs under compressive stress of 6% is carried out solely by carriers with minority spin state, mainly from the nitrogen 2*p* states. Besides, half-metal character can make the electrons with one spin orientation transmitted and the electrons with the other insulated, which is important for spintronics applications. The 100% spin polarization in both F-BNNSs and F-GNNSs under compressive stress of 6% indicates that the half-metal is realized. For F-graphene under stress, different from the variation in F-BNNSs and F-GNNSs, the interaction between the moments keeps AFM coupling independent of the strain (as shown in Fig. 3). Furthermore, the AFM order is strongly more stable than the FM order, which reveals that the AFM spin order in the F-graphene is robust within a wide range of strain. The rapid variation of spin polarization in F-BNNSs, F-GNNSs and F-graphene under strain may find applications in nanodevices, such as a mechanical switch for spin-polarized transport.

3.3 Origin of the magnetic coupling and transition

Understanding of the interesting transition between FM and AFM orders with strain is sought in the magnetic mechanism. According to the currently accepted magnetic mechanisms of half-decorated 2D sheets, the magnetic coupling is ferromagnetism.[19–22] It seems that this mechanism also well hold for the magnetism of F-GNNSs without strain. Yet, for F-GNNSs under tensile stress of 6%, the coupling between the spins is AFM, which can not be explained by these magnetic mechanisms. It is also confirmed that F-graphene and F-BNNSs are AFM semiconductors, which also can not be explained by the currently existing mechanisms. These reveal that the convention mechanisms are not credible in these systems. This of course raises the question as to the previous theoretical results which are

analyzed under the assumption that magnetism arises from these magnetic mechanisms, thus they should be re-examined. Here, we propose a new mechanism that can provide a concise physical understanding of the magnetism of F-BNNSs, F-GNNSs and F-graphene. We find that the magnetism can be determined by the competition of two distinct interactions: (a) through-bond interaction and (b) *p–p* direct interaction. For through-bond interaction, as illustrated in Fig. 1b, it is defined that an atom with up-spin (down-spin) density induces a down-spin (up-spin) density on the adjacent atom directly bonded to it, which may led to FM spin coupling even in long range. In fact, this mechanism of magnetic coupling has also been found for the cation-vacancy induced magnetism in GaN by previous research.[31] Provided that *b*(*i*) and *b*(*j*) represent the *b* atoms at sites *i* and *j*, respectively, the through-bond spin polarization takes place along each *b*(*i*)–(*a*–*b*)*n*–*a*–*b*(*j*) ($n = 0, 1, 2,\ldots$) path. For all the *b*–*b* coupling, each *b*(*i*)–(*a*–*b*)*n*–*a*–*b*(*j*) path consists of an even number of *a*–*b* bonds. Consequently, as illustrated in Fig. 1b, the through-bond spin polarization couples ferromagnetically the spins of the dangling bonds of *b* atoms. Besides, since the valence electrons in *p*-states are more delocalized (as illustrated in Fig. 2), they have much larger spatial extension that promotes direct magnetic coupling interactions between two neighboring *b* atoms (denoted as *p–p* direct interaction). For the *p–p* direct interaction, it is defined that a *b* atom with up-spin (down-spin) density induces a down-spin (up-spin) density on the nearest-neighboring *b* atom directly (as shown in Fig. 1c), without mediated by *a* atom. Provided that *b*(*i*) and *b*(*j*) represent the *b* atoms at sites *i* and *j*, respectively, the *p–p* direct spin polarization takes place along each *b*(*i*)–(*b*)*n*–*b*(*j*) ($n = 0, 1, 2,\ldots$) path. Consequently, as illustrated in Fig. 1c, the *p–p* direct spin polarization couples antiferromagnetically the spins of the dangling bonds of *b* atoms. Although the effects of through-bond and *p–p* direct interactions are the same thing from the viewpoint of bonding theory, the through-bond spin polarization is an indirect interaction mediated by *a* atom, while *p–p* direct spin polarization is an direct interaction through space. Two interactions may be available together.

Based on this mechanism, the magnetism of F-BNNSs, F-GNNSs and F-graphene can be easily understood. For F-BNNSs and F-graphene, the effect of *p–p* direct interaction is more important to determine the magnetic property of the ground state, resulting in antiferromagnetic F-BNNSs and F-graphene. While for F-GNNSs, the interaction between the magnetic moments is mainly determined by the effect of through-bond spin polarization, resulting in ferromagnetic F-GNNSs. The reliability of this mechanism is also well reflected by the variation in the energy difference with strain, which would be discussed in the following. More importantly, this mechanism obtained based on F-BNNSs, F-GNNSs and F-graphene may also well hold for the magnetism of all the previous studied half-fluorinated 2D systems.

Based on this mechanism, we can also understand the evolution of the magnetic properties of F-BNNSs, F-GNNSs and F-graphene with strain, together with the FM-AFM transition behavior. Evidently, the through-bond and *p–p* direct interactions depend sensitively on the strain (as shown in Fig. 3), due to the fact that the distance between two neighboring *b* atoms (d_{b-b}) increases with increasing tensile strain (or decreasing compression strain), and the elongating of d_{b-b} results in the reduction in the spin coupling between magnetic moments. As a results, both through-bond and *p–p* direct interactions decrease with increasing tensile strain (or decreasing compression strain). However, the decrease of the through-bond interaction is larger than that of the *p–p* direct interaction with increasing tensile strain (or decreasing compression strain), resulting in the relative increase of the *p–p* direct interaction. This is why the energy difference ΔE increases monotonically with increasing isotropic strain from −6% to 6% for F-BNNSs, F-GNNSs and F-graphene. This is also responsible for the intriguing strain-depended FM-AFM transitions for F-BNNSs and F-GNNSs. Besides, given the success in explaining the strain effects on F-BNNSs, F-GNNSs and F-graphene in terms of FM-AFM transition can also verify that the magnetism of F-BNNSs, F-GNNSs and F-graphene arises from the combined effects of both through bond and *p–p* direct spin polarizations. These results also have potential implication for many bistable devices utilizing nanosheets where the strain change is expected to significantly alter the magnetic behavior important to their application.

IV. Summary

In summary, systematic first-principles calculations were carried out on half-fluorinated single layers of BN, GaN and graphene, in the context of intercoupling between isotropic strain and magnetic property. Our results reveal that the energy difference between the ferromagnetic spin order and antiferromagnetic spin order increases monotonically with increasing isotropic strain from −6% to 6% for half-fluorinated BNNSs, GNNSs and graphene. Based on the results, we demonstrate that:

(1) The transitions between FM and AFM orders of half-fluorinated BNNSs and GNNSs can conversely be controlled by applying strain: FM semiconductors under compressive stress of 6%, while AFM semiconductors under tensile stress of 6%. Thus controlling the applied strain can precisely modulate the magnetic properties of the half-fluorinated BN and GaN sheets, which endues the half-fluorinated BN and GaN sheets with great potential applications in future functional nanodevices.

(2) We proposed an interesting mechanism that the magnetism of half-fluorinated BNNSs, GNNSs and graphene arises from the combined effects of both through-bond and *p–p* direct interactions. If the interaction between the magnetic moments is mainly contributed by the effect of through-bond spin polarization (or *p–p* direct spin polarization), the coupling is FM (or AFM). And the through-bond and *p–p* direct interactions depend sensitively on the strain.

Further experimental studies are expected to confirm the attractive predications.

Acknowledgements

This work is supported by the National Natural Science foundation of China under Grant 10774091 and 20973102, National Basic Research Program of China (973 Program, Grant No. 2007CB613302).

References

1 T. L. Makarova, B. Sundqvist, R. Hohne, P. Esqulnazl, K. Kopelevich, P. Scharff, V. A. Davydov, L. A. Kahsevarova and A. V. Rakhmanina, *Nature*, 2001, **413**, 716.

2 Y. Shibayama, H. Sato, T. Enoki and M. Endo, *Phys. Rev. Lett.*, 2000, **84**, 1744.
3 J. Fernandez-Rossier and J. J. Palacios, *Phys. Rev. Lett.*, 2007, **99**, 177204.
4 Z. K. Zhang, Y. Dai, B. B. Huang and M.-H. Whangbo, *Appl. Phys. Lett.*, 2009, **96**, 062505.
5 P. O. Lehtinen, A. S. Foster, A. Ayuela, A. Krasheninnikov, K. Nordlund and R. M. Nieminen, *Phys. Rev. Lett.*, 2003, **91**, 017202.
6 A. N. Andriotis, M. Menon, R. M. Sheetz and L. Chernozatonskii, *Phys. Rev. Lett.*, 2003, **90**, 026801.
7 P. O. Lehtinen, A. S. Foster, Y. Ma, A. V. Krasheninnikov and R. M. Nieminen, *Phys. Rev. Lett.*, 2004, **93**, 187202.
8 Y. Zhang, S. Talapatra, S. Kar, R. Vajtai, S. K. Nayak and P. M. Ajayan, *Phys. Rev. Lett.*, 2007, **99**, 107201.
9 K. W. Lee and C. E. Lee, *Phys. Rev. Lett.*, 2006, **97**, 137206.
10 Z. Zhang and W. J. Guo, *J. Am. Chem. Soc.*, 2009, **131**, 6874.
11 F. Li, Z. Zhu, X. Yao and G. Lu, *Appl. Phys. Lett.*, 2008, **92**, 102515.
12 J. Zhou, Q. Wang, Q. Sun and P. Jena, *Phys. Rev. B: Condens. Matter Mater. Phys.*, 2010, **81**, 085442.
13 Y. Son, M. L. Cohen and S. G. Louie, *Nano Lett.*, 2007, **7**, 3518–3522.
14 Z. M. Liao, Y. D. Li, J. Xu, J. M. Zhang, K. Xia and D. P. Yu, *Nano Lett.*, 2006, **6**, 1087.
15 Z. Y. Wang, B. B. Huang, L. Yu, Y. Dai, P. Wang, X. Qin, X. Zhang, J. Wei, J. Zhan, X. Y. Jing, H. Liu and M.-H. J. Whangbo, *J. Am. Chem. Soc.*, 2008, **130**, 16366.
16 Y. D. Ma, Y. Dai and B. B. Huang, *Comput. Mater. Sci.*, 2011, **50**, 1661.
17 J. O. Sofo, A. Chaudhari and G. D. Barber, *Phys. Rev. B: Condens. Matter Mater. Phys.*, 2007, **75**, 153401.
18 D. C. Elias, R. R. Nair, T. M. G. Mohiuddin, S. V. Morozov, M. P. Blake, P. Halsall, A. C. Ferrari, D. W. Boukhvalov, M. I. Katsnelson, A. K. Geim and K. S. Novoselov, *Science*, 2009, **323**, 610.
19 J. Zhou, Q. Wang, Q. Sun, X. S. Chen, Y. Kawazoe and P. Jena, *Nano Lett.*, 2009, **9**, 3867.
20 B. Xu, J. Yin, Y. D. Xia, X. G. Wan and Z. G. Liu, *Appl. Phys. Lett.*, 2010, **96**, 143111.
21 E. J. Kan, H. J. Xiang, F. Wu, C. Tian, C. Lee, J. L. Yang and M.-H. Whangbo, *Appl. Phys. Lett.*, 2010, **97**, 122503.
22 J. Zhou, M. M. Wu, X. Zhou and Q. Sun, *Appl. Phys. Lett.*, 2009, **95**, 103108.
23 J. P. Perdew, K. Burke and M. Ernzerhof, *Phys. Rev. Lett.*, 1996, **77**, 3865.
24 G. Kresse and J. Furthmuller, *Phys. Rev. B: Condens. Matter*, 1996, **54**, 11169.
25 G. Kresse and J. Joubert, *Phys. Rev. B*, 1999, **59**, 1758.
26 H. J. Monkhorst and J. D. Pack, *Phys. Rev. B: Solid State*, 1976, **13**, 5188.
27 H. Sahin, S. Cahangirov, M. Topsakal, E. Bekaroglu, E. Akturk, R. T. Senger and S. Ciraciprb, *Phys. Rev. B: Condens. Matter Mater. Phys.*, 2009, **80**, 155453.
28 J. Meyer, A. Chuvilin, G. Algara-Siller, J. Biskupek and U. Kaiser, *Nano Lett.*, 2009, **9**, 2683.
29 Y. Ding and J. Ni, *Appl. Phys. Lett.*, 2009, **95**, 083115.
30 H. Peng, H. Xiang, S. Wei, S. Li, J. Xia and J. Li, *Phys. Rev. Lett.*, 2009, **102**, 017201.
31 H. Jin, Y. Dai, B. B. Huang and M.-H. Whangbo, *Appl. Phys. Lett.*, 2009, **94**, 162505.
32 S. A. Wolf, D. D. Awschalom, R. A. Buhrman, J. M. Daughton, S. von Molnar, M. L. Roukes, A. Y. Chtchelkanova and D. M. Treger, *Science*, 2010, **294**, 1488.
33 S.-M. Choi, S.-H. Jhi and Y.-W. Son, *Phys. Rev. B: Condens. Matter Mater. Phys.*, 2010, **81**, 081407.
34 M. Zhou, Y. H. Lu, C. Zhang and Y. P. Feng, *Appl. Phys. Lett.*, 2010, **97**, 103109.

